

## Determination of internal strain by optical measurements

H.-J. Weber

*Universität Dortmund, D-44221 Dortmund, Germany*

(Received 5 December 1994)

Strain-induced atomic displacements can be determined by diffraction experiments only in the case of extraordinarily favorable conditions. I propose optical measurements as an alternative method for determining components of internal strain. Based on the bond-charge model, optical and structural quantities are related by bond parameters. They are obtained from the optical constants of selected materials. Then, internal displacements are determined by piezo-optical measurements. The method is demonstrated with the bonds Ge—O and Si—O and its reliability is tested. Its sensitivity is six orders of magnitude higher than the sensitivity obtained in diffraction experiments.

### I. INTRODUCTION

In a crystal a macroscopic strain  $\epsilon_{ij}$  causes two kinds of atomic displacements  $u_i$ . If the atomic positions with respect to the edges of the unit cell do not change during the deformation the displacements are homogeneous. They are given by

$$u_i^{(\lambda)} = \epsilon_{ij} r_j^{(\lambda)}, \quad (1a)$$

where  $r_j^{(\lambda)} = x_j^{(\lambda)} a_j^{(\lambda)}$  is the position of the atom labeled “ $\lambda$ ” in the unit cell. Obviously the homogeneous displacements defined in Eq. (1a) can be calculated by using the relative coordinates  $x_i$  and the lattice constants  $a_i$ . If atoms do not occupy a center of symmetry additional  $u_i$ 's are induced.<sup>1</sup> This phenomenon, called “internal strain,” is associated with the change of relative coordinates which cannot be calculated in a simple way. Such internal displacements are involved in elasticity, piezoelectricity, different spectroscopic effects,<sup>2</sup> and in theories considering lattice vibrations.<sup>3</sup> Thus, a quantitative understanding of various phenomena on an atomistic level needs the knowledge of internal strain. The additional displacements are described by the tensor  $\vec{A}$  which is defined by the second term in<sup>4-6</sup>:

$$u_i^{(\lambda)} = \epsilon_{ij} r_j^{(\lambda)} + A_{ijk}^{(\lambda)} \epsilon_{jk}. \quad (1b)$$

The nonvanishing components  $A_{ijk}$  are given by the site symmetry of the atoms in the unit cell. In a complex crystal each sublattice may have its own tensor  $\vec{A}$ . For some structures  $\vec{A}$  has been considered theoretically.<sup>7-9</sup> We have derived the components of  $\vec{A}$  in the following way. At first all symmetry operations which are not destroyed by the strain are determined by direct inspection. They specify the space group of the strained crystal. In a second step the atomic positions in the old and in the new space group are inspected using the International Tables for Crystallography.<sup>10</sup> This comparison reveals the relative coordinates which are changed by  $\epsilon_{ij}$ .

An appropriate experimental technique for determining internal strain seems to be a measurement of the intensity of x rays diffracted by an uniaxially stressed crystal.<sup>11,12</sup> However, in the past this method worked only

with Si (Refs. 4, 13, and 14) and Ge,<sup>4,15</sup> both showing the diamond structure. In these materials the uniaxial stress creates a Bragg reflection which is forbidden otherwise. Therefore, it can be detected rather easily. For GaAs reported results are contradictory.<sup>16-18</sup> Cousins<sup>18</sup> found that the impact of uniaxial stresses on extinction effects dominates the changes of diffracted intensities and prevents a determination of internal strain. In general the relative change of diffracted intensity is smaller than in GaAs. Thus, in spite of its fundamental importance, the experimental determination of internal strain is an unsolved problem and techniques which are alternative to x-ray diffraction are needed.

In the present work we propose piezo-optical measurements as a sensitive tool for the determination of internal strain. We use Phillips<sup>19</sup> and Van Vechten's<sup>20</sup> bond-charge model to connect the optical susceptibility  $\chi$  to structural parameters. In the past it was successfully applied in theories on nonlinear optical<sup>21</sup> and electro-optical effects.<sup>22</sup> The most important idea of the dielectric theory is to describe  $\chi$  in terms of the bond polarizabilities  $\beta$ . The  $\beta$ 's are empirical parameters. For birefringent crystals Chemla<sup>23</sup> suggested the use of two different bond parameters, the longitudinal polarizability  $\beta^L$  and the transverse polarizability  $\beta^T$ . It is more convenient to use average and anisotropic quantities which are defined by  $\bar{\beta} = (\beta^L + 2\beta^T)/3$  and  $\Delta\beta = 2(\beta^L - \beta^T)/3$ . Chemla<sup>23</sup> has also stressed the importance of the local field factor  $F$  and Shih and Yariv<sup>22</sup> have pointed out the dependence of bond polarizabilities on the bond length  $d$ . In a birefringent crystal the difference of two susceptibilities can be as small as  $10^{-3}$ . To relate optical and structural quantities on such a high level of sensitivity details of the used model get important. In the past we have considered the bond charge model in various dielectric materials.<sup>24-27</sup> The experiences made in these studies are summarized in the following list which specifies the model in some detail.

(1) Each bond is characterized by the two parameters  $\bar{\beta}$  and  $\Delta\beta$  and their dependence on the bond length  $d$ :<sup>22</sup>

$$\bar{\beta}(d) = \bar{\beta} \left[ 1 + \bar{f} \frac{d - d_R}{d_R} \right], \quad (2a)$$

$$\Delta\beta(d) = \Delta\beta \left[ 1 + \Delta f \frac{d - d_R}{d_R} \right], \quad (2b)$$

where  $d_R$  is the bond length to which  $\bar{\beta}$  and  $\Delta\beta$  are referred.

(2) Assuming that the total bond charge is the same for different coordination numbers  $N$ , the dependence of  $\beta$  ( $\bar{\beta}$  as well as  $\Delta\beta$ ) on  $N$  can be expressed by<sup>28</sup>

$$\beta \propto \frac{Z_A}{N_A} + \frac{Z_B}{N_B}, \quad (3)$$

where  $Z_A$  and  $Z_B$  are the bond charge contributions of the cation  $A$  and of the anion  $B$ , respectively.

(3) The local field factor is approximated by the Lorentz term

$$\bar{F} = 1 + \frac{\bar{\chi}}{3}, \quad (4)$$

where  $\bar{\chi} = (\chi_{11} + \chi_{22} + \chi_{33})/3$  is the average optical susceptibility.

(4) The model works well only for vanishing photon energies.

Assuming that the macroscopic polarization of a crystal is the density of the microscopic dipoles induced by a light wave,  $\bar{\beta}$  and  $\Delta\beta$  connect optical and structural quantities in a rather simple way as will be shown in Sec. II.

The idea is to evaluate the four parameters  $\bar{\beta}$ ,  $\Delta\beta$ ,  $\bar{f}$ , and  $\Delta f$  of a bond from the refractive indices of selected crystals. Then, internal strain parameters are determined by piezo-optical measurements. In the present work we want to demonstrate that this procedure is reliable. One precondition is the universal character of the bond parameters. This is tested by considering an excess of experimental data in crystals which differ in structural and physical properties as strongly as possible. The method is demonstrated with the example of the Ge—O bond in Sec. III. In Sec. IV the parameters of the Si—O bond are evaluated using data from literature. Parameters of internal strain are given in Sec. V and in Sec. VI we discuss the main difference between the traditional diffraction method and the optical procedure proposed here.

## II. RELATIONS BETWEEN OPTICAL AND STRUCTURAL QUANTITIES

The optical susceptibilities  $\bar{\chi}$  and  $\Delta\chi_{(i)} = \chi_{ii} - \bar{\chi}$  are related to the bond parameters and structural quantities by<sup>26,27</sup>

$$\bar{\chi} = \frac{\bar{F}}{V} \sum_{\mu} [\bar{\beta}(d)]^{\mu}, \quad (5a)$$

$$\Delta\chi_{(i)} = \frac{\bar{F}^2}{2V} \sum_{\mu} [\Delta\beta(d)(3C_{(i)}^2 - 1)]^{\mu}. \quad (5b)$$

The index “ $\mu$ ” enumerates the bonds within one unit cell of volume  $V$ . The atomic positions are involved in  $C_{(i)} = (x^B - x^A)_i a_i / d$  where  $(x^B - x^A)_i$  is the difference of the relative coordinates of the two atoms in the bond  $A-B$ .

Equation (5a) shows that  $\bar{\chi}$  does not depend on

structural details. In Eq. (5b), however, each term of the sum can be positive or negative. As a consequence,  $\Delta\chi_{(i)}$  reflects the structural parameters in a very sensitive way. It is convenient to distinguish between two kinds of structural anisotropies. The first describes the anisotropy of bond orientations:

$$G_{(i)} = \sum_{\mu} [3C_{(i)}^2 - 1]^{\mu}. \quad (6a)$$

The second represents the anisotropy of the bond length:

$$D_{(i)} = \sum_{\mu} \left[ (3C_{(i)}^2 - 1) \frac{d - d_R}{d_R} \right]^{\mu}. \quad (6b)$$

With above abbreviations the quantity

$$\Delta\chi_{(i)}^* = \Delta\chi_{(i)} \frac{2V}{\bar{F}^2} \quad (7a)$$

is given by

$$\Delta\chi_{(i)}^* = \sum_{\nu} [G_{(i)} \Delta\beta + D_{(i)} \Delta\beta \Delta f]^{\nu}, \quad (7b)$$

where the index  $\nu$  denotes different types of bonds.

In Eqs. (1)–(7)  $\bar{\chi}$  and  $\Delta\chi_{(i)}$  are tensor invariants<sup>29</sup> and Cartesian tensor components are labeled by indices which are not in parentheses. In the following text the latter will be used in the matrix notation.<sup>30</sup> The piezo-optical experiments were performed with uniaxial stresses  $\sigma_i$ , but for the theoretical description the dependence on strain  $\epsilon_i$  is preferred. We define the increment of the optical susceptibility

$$\chi_i - \chi_i^{(0)} = q_{ij} \sigma_j = q_{ij} c_{jk} \epsilon_k, \quad (8)$$

where  $c_{ij}$  are the elastic constants.

At first we consider strains which are parallel to the axes of coordinates. Differentiating Eqs. (5)–(7) with respect to the strain  $\epsilon_i$  ( $i = 1, 2, 3$ ) we obtain

$$\frac{\delta(\bar{\chi})}{\delta\epsilon_j} = -\bar{\chi} \bar{F} \frac{\delta \ln V}{\delta\epsilon_j} + \frac{\bar{F}^2}{V} \sum_{\mu} \left[ \bar{\beta} \bar{f} \frac{\delta \ln d}{\delta\epsilon_j} \right]^{\mu}, \quad (9a)$$

$$\frac{\delta(\Delta\chi_{(i)})}{\delta\epsilon_j} = \Delta\chi_{(i)} \left[ \frac{2}{3\bar{F}} \frac{\delta\bar{\chi}}{\delta\epsilon_j} - \frac{\delta \ln V}{\delta\epsilon_j} \right] + \frac{\bar{F}^2}{2V} \frac{\delta(\Delta\chi_{(i)}^*)}{\delta\epsilon_j}, \quad (9b)$$

$$\frac{\delta(\Delta\chi_{(i)}^*)}{\delta\epsilon_j} = \sum_{\mu} \left[ 6C_{(i)} \frac{\delta C_{(i)}}{\delta\epsilon_j} \Delta\beta + (3C_{(i)}^2 - 1) \frac{\delta \ln d}{\delta\epsilon_j} \Delta\beta \Delta f \right]^{\mu}. \quad (9c)$$

For each bond the influence of the strain is given by

$$\frac{\delta C_{(i)}}{\delta\epsilon_j} = C_{(i)} \left[ \frac{\delta \ln a_i}{\delta\epsilon_j} - \frac{\delta \ln d}{\delta\epsilon_j} \right] + C_{(i)} \frac{\delta \ln x_i}{\delta\epsilon_j}, \quad (10a)$$

$$\frac{\delta \ln d}{\delta\epsilon_j} = C_{(j)}^2 \frac{\delta \ln a_j}{\delta\epsilon_j} + \sum_{k=1}^3 C_{(k)}^2 \frac{\delta \ln x_k}{\delta\epsilon_j}. \quad (10b)$$

In Eqs. (10) the last term denotes the contribution of internal strain.

In the case of a shear strain  $\epsilon_k$  ( $k = 4, 5, 6$ ) we neglect

internal displacements throughout this work. The influence of homogeneous displacements is given by

$$\chi_k = \frac{3\bar{F}}{4V} \sum_{\mu} \Delta\beta(d) [C_{(i)}^2 + C_{(j)}^2 - 4C_{(i)}^2 C_{(j)}^2]^{\mu} \epsilon_k, \quad (11)$$

where  $k = 9 - i - j$ . It should be noted that all equations are referred to a Cartesian system of coordinates. For trigonal and hexagonal crystals (monoclinic and triclinic symmetry is not considered here) atomic coordinates have to be converted before above equations are applicable.

### III. The Ge—O BOND

#### A. Selection of materials

In the present model a bond is characterized by the four parameters  $\bar{\beta}$ ,  $\Delta\beta$ ,  $\bar{f}$ ,  $\Delta f$ . To obtain  $\bar{f}$  and  $\Delta f$ , compounds with a sufficiently strong variation of the bond length are needed. These are compounds with Ge—O bonds because Ge can be surrounded by four or six oxygen atoms and a change of the coordination number  $N_{\text{Ge}}$  is accompanied by a change of the bond length. We have selected tetragonal  $\text{GeO}_2$  and orthorhombic  $\text{K}_2\text{Ge}_8\text{O}_{17}$  (abbreviated KGe) as reference materials for  $N_{\text{Ge}} = 6$  and  $N_{\text{Ge}} = 4$ , respectively. In addition, we have used tetragonal  $\text{Na}_4\text{Ge}_9\text{O}_{20}$  (abbreviated NaGe) which shows both coordination numbers simultaneously. In KGe  $N_{\text{Ge}} = 4$  is dominant but for some Ge atoms the unusual coordination  $N_{\text{Ge}} = 5$  (Ref. 31) is realized. Thus, in these three compounds the Ge—O bonds are arranged in rather different ways. The occurrence of K—O and Na—O bonds as minor components introduces no additional problems because their optical parameters are well known from a previous work.<sup>27</sup>

Growth of single crystals and optical constants of  $\text{GeO}_2$  and  $\text{Na}_4\text{Ge}_9\text{O}_{20}$  were reported previously.<sup>32</sup> The refinement of the structure and some thermal properties of  $\text{K}_2\text{Ge}_8\text{O}_{17}$  have been published recently.<sup>33</sup> Refractive indices of  $\text{K}_2\text{Ge}_8\text{O}_{17}$  we have determined in the visible spectral range by the prism method. The results of refractive index measurements were used for evaluating the average susceptibility  $\bar{\chi} = \bar{n}^2 - 1$ . For all three crystals the dispersion of  $n$  shows that transitions with large oscillator strength are centered near 10 eV. This is in accordance with band-structure calculations for rutile compounds.<sup>34</sup> The values of  $\bar{\chi}$  were obtained at significantly smaller photon energies (1.6–3.3 eV). Therefore,  $\bar{\chi}$  can be expanded in the power series

$$\bar{\chi}(E) = \bar{\chi} + \bar{\chi}^{(1)} E^2 + \dots, \quad (12)$$

where  $E = \hbar\omega$  is the photon energy. Results for  $E = 0$  are given in Table I together with some crystallographic data.  $\bar{\chi}$  is nearly the same for KGe and NaGe, but it is significantly larger for  $\text{GeO}_2$ .

#### B. Spontaneous and induced birefringence

Whereas  $\bar{\chi}$  reflects average properties of materials, the difference

TABLE I. Structural and optical data of germanates. The optical contributions of Na—O and K—O bonds are given in parentheses.  $V$  is the volume of a unit cell and  $\bar{d}$  is the average length of the Ge—O bonds.

	$\text{GeO}_2$	$\text{Na}_4\text{Ge}_9\text{O}_{20}$	$\text{K}_2\text{Ge}_8\text{O}_{17}$
Space group	$P4_2/mnm$	$I4_1/a$	$Pnam$
$V$ ( $\text{\AA}^3$ )	55.36	1657	1557
$\bar{d}$ ( $\text{\AA}$ )	1.882	1.831	1.797
$\bar{\chi}$	2.837	1.79 (15.6%)	1.785 (9.1%)
$\Delta\chi_{(3)}$	0.229	0.025 (0.0%)	−0.008 (9.0%)
$\Delta\chi_{(1)}$			−0.0123 (2.8%)

$$\chi_i - \chi_j = 2\bar{n}(n_{(i)} - n_{(j)})$$

depends more sensitively on electronic details. Therefore, the birefringence

$$\delta = \frac{2\pi}{\lambda} (n_{(i)} - n_{(j)})L$$

of thin plates with thickness  $L$  was determined in a large spectral range. Measurements were performed with a scanning wavelength method.<sup>27</sup> Figure 1 presents the results for  $\chi_i - \chi_j$  as a function of the squared photon energy. For NaGe and KGe there is always a sufficiently large linear range which is used for determining the susceptibility at  $E = 0$ . At small photon energies most curves show the influence of IR bands. Their presence in the  $\text{GeO}_2$  spectrum has been eliminated with aid of IR data.<sup>35</sup> The residual spectrum was fitted by using, in addition to the first terms of a power series, a simple resonance term. The fit yielded a resonance energy of 4.74 eV which is close to the position of the direct forbidden band gap at 4.68 eV.<sup>36</sup> The values obtained for  $E = 0$  from the fits in Fig. 1 are listed in Table I. Note, that the average contribution of Na—O and K—O is only 10% of the total values.

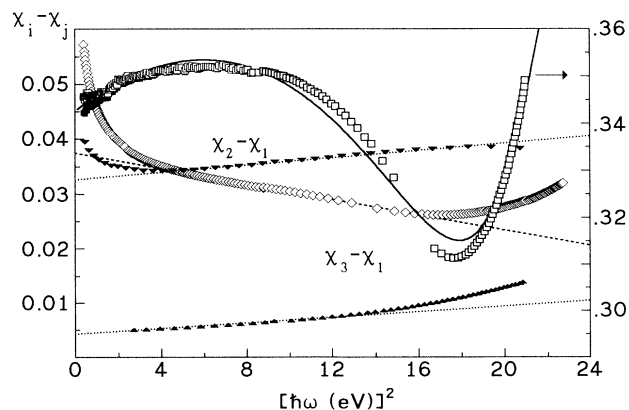


FIG. 1. Difference of optical susceptibilities in  $\text{GeO}_2$  (solid squares are raw data, in open squares IR influences are eliminated),  $\text{Na}_4\text{Ge}_9\text{O}_{20}$  (diamonds), and  $\text{K}_2\text{Ge}_8\text{O}_{17}$  (triangles). Lines are least-squares fits as explained in the text.

Piezo-optical coefficients were determined in rectangular samples of  $\text{GeO}_2$  and  $\text{KGe}$  by recording the birefringence  $\delta$  as a function of uniaxial stresses. Using a He-Ne laser ( $\lambda=633$  nm,  $E^2=3.8$  eV<sup>2</sup>) the influence of dispersion effects are small (see Fig. 1). Applying alternating stresses (frequency about 120 Hz) the changes of  $\delta$  were detected by lock-in techniques. A typical result is shown in Fig. 2. Over more than three orders of magnitude the induced birefringence depends linearly on stress. The piezo-optical results are presented in Table II. To convert these coefficients in elasto-optical ones, the elastic constants are needed as in Eq. (8). For  $\text{GeO}_2$  they have been reported previously.<sup>37</sup> In  $\text{KGe}$  we have determined the  $c_{ij}$  by measuring the resonance frequencies of ultrasonic waves propagating in rectangular samples. These results are added to Table II. The longitudinal elastic constants are larger in  $\text{GeO}_2$  by a factor 6. Thus, the elastic as well as the optical susceptibilities are significantly different for both crystals.

### C. Bond parameters

In Eqs. (5)–(7) optical and structural quantities are linearly connected. Figure 3 demonstrates that optical anisotropy obeys the predicted linearity with high accuracy. The same is observed for average optical susceptibilities. The bond parameters derived from these results are presented in Table III.

In a next step we have to clarify that the parameters observed in unstressed crystals are valid in stressed crystals, too. Evidence for this identity is given if elasto-optical effects are described by Eqs. (9)–(11) with a vanishing internal strain. This approximation is supposed to be most likely for shear strains, because such strains do not change the volume. Indeed,  $\delta\chi_6/\delta\epsilon_6$  in  $\text{GeO}_2$  and in  $\text{KGe}$  behave as expected. This is demonstrated in Fig. 3 by the two values represented by diamonds. They were obtained by changing the experimental results for  $\delta\chi_6/\delta\epsilon_6$  by use of Eq. (11) into a form which is appropriate for a common representation with natural anisotropy

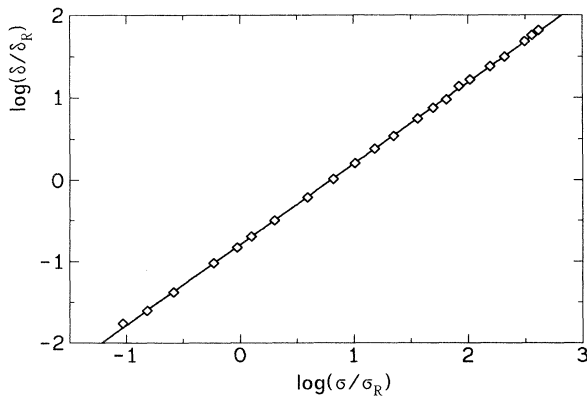


FIG. 2. Double logarithmic plot (to base 10) of stress-induced birefringence  $\delta$  versus the modulation amplitude  $\sigma$  of uniaxial stress in  $\text{KGe}$ . Length of the sample is 4.4 mm. Reference values are  $\delta_R=10^{-3}$  rad and  $\sigma_R=10^3$  Pa.

TABLE II. Piezo-optical constants  $q_{ij}=\delta\chi_i/\delta\sigma_j$  (unit  $10^{-12}$  Pa<sup>-1</sup>) in  $\text{GeO}_2$  and  $\text{K}_2\text{Ge}_8\text{O}_{17}$  and the elastic constants  $c_{ij}$  (unit  $10^9$  Pa) of  $\text{K}_2\text{Ge}_8\text{O}_{17}$ . Uncertainties are given in parentheses.

$\text{GeO}_2$	$\text{K}_2\text{Ge}_8\text{O}_{17}$	$\text{K}_2\text{Ge}_8\text{O}_{17}$
$q_{11}-0.96q_{31}=14.7(1.7)$	$q_{11}-q_{21}=16.5(1.4)$	$c_{11}=65.9(0.7)$
$q_{12}-0.96q_{31}=19.5(3.3)$	$q_{11}-q_{31}=12.5(0.8)$	$c_{22}=87.3(1.0)$
$q_{33}-1.04q_{13}=5.1(1.2)$	$q_{22}-q_{12}=18.9(1.8)$	$c_{33}=56.2(0.4)$
	$q_{22}-q_{32}=18.8(1.7)$	$c_{12}=26(1)$
	$q_{33}-q_{13}=13.6(3.3)$	$c_{13}=9(1)$
	$q_{33}-q_{23}=17.9(2.4)$	$c_{23}=19(1)$
		$c_{44}=4.8(0.1)$
		$c_{55}=20.6(0.1)$
		$c_{66}=12.8(0.1)$

as shown in Fig. 3. We try the same approach also with  $\epsilon_i$  along the main axes. In Fig. 4 the experimental values are compared with those calculated for a vanishing internal strain. Only  $\delta(\Delta\chi_3)/\delta\epsilon_1$  and  $\delta(\Delta\chi_3)/\delta\epsilon_3$  for  $\text{GeO}_2$  and  $\delta(\Delta\chi_2)/\delta\epsilon_2$  and  $\delta(\Delta\chi_3)/\delta\epsilon_2$  for  $\text{KGe}$  show a finite value for internal strain which is clearly larger than the experimental uncertainty. The majority of elasto-optical coefficients in Fig. 4 and the two values in Fig. 3 are consistent with the absence of internal strain and the identity of bond parameters in unstressed and stressed crystals.

### IV. THE Si—O BOND

Si—O can be considered as one of the most important bonds in inorganic chemistry. As silicates are the main constituents of rock forming minerals, their optical properties have been extensively studied. Nevertheless, the evaluation of  $\bar{f}$  and  $\Delta f$  is more difficult than in the case of Ge—O because the bond length  $d_{\text{Si—O}}$  is rather constant in different minerals. We have chosen the Si—O bond as a second example because in  $\alpha\text{-SiO}_2$  internal displacements have been determined by neutron diffraction.<sup>38</sup> This enables a consistency check between optical and diffraction methods. The experiment was performed with hydrostatic pressure  $p_0$ . In contrast to uniaxial stresses  $\sigma_i$  a hydrostatic pressure yields reliable diffraction results because  $p_0$  can be much larger than  $\sigma_i$ . In  $\alpha\text{-SiO}_2$   $p_0$  was about  $10^9$  Pa.<sup>38</sup> With this pressure the changes of the four relative coordinates<sup>39</sup> were determined with an error of 35%. Using the reported structural results together with the elastic and elasto-optical constant of  $\alpha\text{-SiO}_2$ ,<sup>40</sup>  $\delta\bar{\chi}/\delta p_0$ , and  $\delta\Delta\chi_{(3)}/\delta p_0$  are obtained in terms of  $\bar{\beta}$ ,  $\bar{f}$  and  $\Delta\beta$ ,  $\Delta f$ , respectively. In Fig. 5 the anisotropic part of the result is presented as  $\Delta\chi_{hs}$ .

TABLE III. Optical parameters of the bonds Si—O and Ge—O. Values are referred to the coordination number  $N_R=4$  and to the bond length  $d_R$ . Units are  $\text{\AA}$  ( $d_R$ ) and  $\text{\AA}^3$  ( $\bar{\beta}$ ,  $\Delta\beta$ ).

	$d_R$	$\bar{\beta}$	$\Delta\beta$	$\bar{f}$	$\Delta f$
Si—O	1.604	9.00(20)	9.66(8)	1.17(2)	0.57(2)
Ge—O	1.74	12.81(19)	5.22(4)	-2.66(4)	-1.13(8)

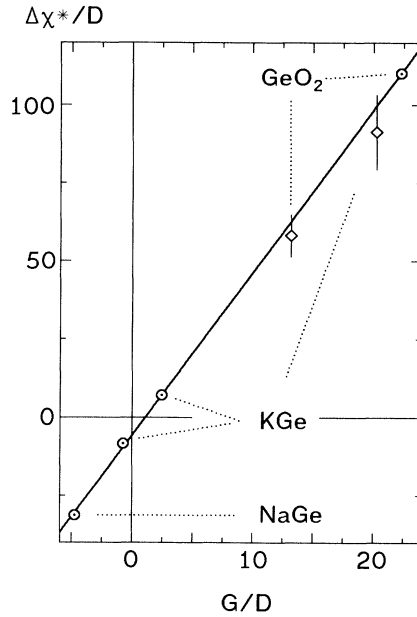


FIG. 3. Optical anisotropy (circles) in crystals with Ge—O bonds versus structural parameters.  $\Delta\chi^*$ ,  $G$ , and  $D$  are defined in Eqs. (6) and (7). Diamonds represent results which are derived from the elasto-optical effect  $\delta\chi_6/\delta\epsilon_6$ . Solid line is least-squares fit. The slope gives  $\Delta\beta$  and the  $y$ -axis intercept is  $\Delta\beta\Delta f$ .

A second photoelastic value, denoted by  $\chi_{ss}$  in Fig. 5 is evaluated from the average  $(\delta\chi_4/\delta\epsilon_4 + \delta\chi_6/\delta\epsilon_6)/2$  by use of Eq. (11). Furthermore, two values which represent the bond parameters in mechanically free materials are ob-

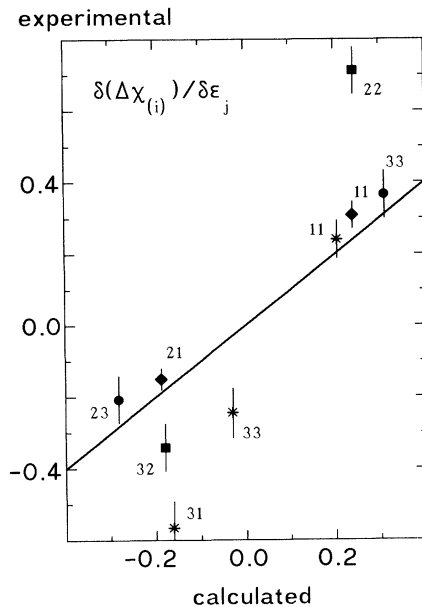


FIG. 4. A comparison of experimental and calculated (without internal strain) elasto-optical coefficients in KGe (squares, circles, diamonds) and  $\text{GeO}_2$  (stars). The given numbers  $ij$  indicate directions in the measurement of  $\delta(\Delta\chi_{(i)})/\delta\epsilon_j$ . The values for  $\text{GeO}_2$  are ten times bigger than shown in the figure. The solid line illustrates the 1:1 correspondence.

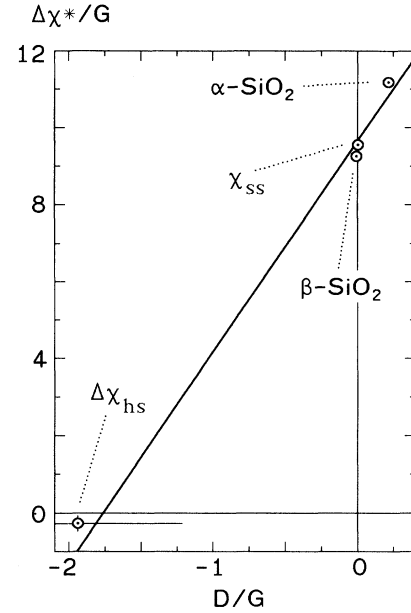


FIG. 5. Optical anisotropy versus structural parameters for Si—O bonds. Values denoted by  $\alpha\text{-SiO}_2$  and  $\beta\text{-SiO}_2$  are obtained from birefringence of the low- and the high-temperature modification of quartz.  $\Delta\chi_{ss}$  and  $\Delta\chi_{hs}$  are derived from elasto-optical effects as described in the text. The solid line represents a least-squares fit.

tained from the natural birefringence of trigonal  $\alpha\text{-SiO}_2$  and of hexagonal  $\beta\text{-SiO}_2$ .<sup>40</sup> The solid line in Fig. 5. represents a least-squares fit of the two parameters  $\Delta\beta$  and  $\Delta\beta\Delta f$  for the Si—O bond. In evaluating  $\Delta\chi_{hs}$  diffraction results were used. They are obviously consistent with the optical data. The parameters  $\bar{\beta}$  and  $\bar{f}$  are obtained from  $\bar{\chi}$  of both compounds and from  $\delta\bar{\chi}/\delta p_0$  of  $\alpha\text{-SiO}_2$ . All results are summarized in Table III.

## V. COMPONENTS OF INTERNAL STRAIN

Based on the two sets of bond parameters in Table III, structural changes can be determined from the results of piezo-optical experiments. In  $\text{K}_2\text{Ge}_8\text{O}_{17}$  internal strain was observed only for  $\epsilon_i$  parallel to the  $b$  axis (see Fig. 4). The special importance of this axis (pseudotetragonal axis) is clearly visible in the structure of KGe (Ref. 33) and manifests itself in optical and elastic properties, too (see Tables I and II). This qualitative agreement in the anisotropy of different properties is the only result for KGe. As the number of free structural parameters is 44, we have no chance to obtain their dependence on strain.

The rutile structure of  $\text{GeO}_2$  shows one free structural parameter, which is the  $x_1(x_2=x_1)$ -coordinate of the oxygen atom.<sup>41</sup> For a strain along the  $c$  axis only this relative coordinate varies, which is described by the component  $A_{13}$  of the tensor of internal strain. The strain  $\epsilon_1$  destroys the fourfold axis and the original space group  $P4_2/mnm$  [No. 136 of the International Tables for X-ray Crystallography (Ref. 10)] is changed to  $P2_1/mnm$  (No. 58). In this orthorhombic space group the two Ge atoms

of the unit cell and the  $x_3$  component of the O atoms are the same as before. The  $x_1$  and  $x_2$  components of O, which are connected in the rutile structure are now independent from each other. Thus, for  $\epsilon_1$  two parameters of internal strain exist. The sketched analysis is easily continued for shear strains. Finally we obtain the matrix for the internal displacements of O given in Table IV. For strains along the crystallographic axes the tensor components have been determined by our piezo-optical measurements. Numerical results are given in Table IV. The agreement between the experimental and calculated value for  $\delta\chi_6/\delta\epsilon_6$  (see Fig. 3) shows that  $A_{16}=0$  within the given experimental accuracy. The shear strain  $\epsilon_4$  (or  $\epsilon_5$ ) induces a three-dimensional displacement. It is described by the three tensor components  $A_{14}, A_{24}, A_{34}$ . Unfortunately, the same strain gives only one additional elasto-optical coefficient. Therefore, the three components  $A_{14}, A_{24}, A_{34}$  cannot be determined by piezo-optical measurements alone.

In both crystals, KGe and GeO<sub>2</sub>, the number of components of internal strain is larger than the number of available experimental data. The same problem happens with  $\alpha$ -quartz, too. However, with the example of  $\alpha$ -SiO<sub>2</sub> we can demonstrate that crystal chemical considerations are able to support experimental results. For a stress along the trigonal axis four structural parameters are free to vary, but only two piezo-optical data are available. The gap between available and needed quantities even increases for other directions of stress. Inspecting interatomic distances in a SiO<sub>4</sub> tetrahedron, we notice that out of the six O—O distances three are short (2.605–2.613 Å) and three long (2.636–2.639 Å).<sup>39</sup> Note, that the effective ionic radius of O<sup>2-</sup> derived from a representative number of compounds is  $r_O=1.40$  Å (Ref. 42) to  $r_O=1.375$  Å (Ref. 43). Thus, even the longest O—O distance in  $\alpha$ -SiO<sub>2</sub> is relatively short. As repulsive forces increase strongly with decreasing distance it is very unlikely that the compression  $-\sigma_3$  causes a further decrease of the shortest distances. They should be constant. This restriction allows us to eliminate the variation of two structural parameters. The two remaining variations can be determined by the experimental results for  $\delta\bar{\chi}/\delta\sigma_3$  and  $\delta\Delta\chi_{(3)}/\delta\sigma_3$ . The obtained atomic displacements are given in Table V. A countercheck of this result is performed in the following way. Two Si—O distances in a SiO<sub>4</sub> tetrahedron show  $d_1=1.595$  Å and two bonds show  $d_2=1.613$  Å. Compared with the effective ionic radii of O<sup>2-</sup> and Si<sup>4+</sup> both distances are rather short. Therefore, we expect  $\delta d_2/\delta\sigma_3$  to be significantly bigger than  $\delta d_1/\delta\sigma_3$ . With the result of Table V we obtain

TABLE IV. Matrix of internal strain components for the rutile structure and some numerical values for GeO<sub>2</sub>.

$A_{11}$	$A_{12}$	$A_{13}$	$A_{14}$	$A_{15}$	$A_{16}$
$A_{12}$	$A_{11}$	$A_{13}$	$A_{15}$	$A_{14}$	$A_{16}$
0	0	0	$A_{34}$	$A_{34}$	0

$A_{11}=3.6\pm 1.9$  Å;  $A_{12}=-7.0\pm 2.2$  Å;  $A_{13}=-0.92\pm 0.26$  Å.

TABLE V. Stress-induced changes of relative coordinates in  $\alpha$ -SiO<sub>2</sub> in units of  $10^{-12}$  Pa<sup>-1</sup>. The  $x$  component of Si is denoted by  $u$  and  $x, y, z$  are the relative coordinates of O.

$\delta u/\delta\sigma_3$	$\delta x/\delta\sigma_3$	$\delta y/\delta\sigma_3$	$\delta z/\delta\sigma_3$
-7.3	0.4	1.6	-1.4

$$\delta d_1/\delta\sigma_3 = -1.1 \pm 1.8 (10^{-12} \text{ \AA/Pa}),$$

$$\delta d_2/\delta\sigma_3 = 28.8 \pm 1.8 (10^{-12} \text{ \AA/Pa}),$$

which is very reasonable in the light of above considerations.

## VI. DISCUSSION

All tests demonstrate that the proposed piezo-optical method works reliably. As shown in Sec. V, the number of available piezo-optical data is usually too small for determining all internal displacements. This is the main disadvantage of the method. Its main advantage is the high sensitivity. This is impressively revealed by a comparison of piezo-optical measurements with diffraction experiments. Jorgensen<sup>38</sup> needed a hydrostatic pressure of more than  $10^8$  Pa for detecting internal strain. Figure 2 demonstrates piezo-optical measurements with less than  $10^2$  Pa. The following example will show that the difference in sensitivity of more than six orders of magnitude cannot be decreased significantly by technical improvements. Cousins<sup>12</sup> suggested the use of synchrotron radiation and modulation techniques to measure internal strain as sensitively as possible. Such an experiment was recently reported by Graafsma *et al.*<sup>44</sup> They measured electric-field-induced displacements in 2-methyl-4-nitroaniline (MNA) which shows an extremely large piezoelectrical effect. Relative changes of  $10^{-3}$  were detected with an accuracy of 20%. The sensitivity was significantly higher than in the experiment of Jorgensen,<sup>38</sup> most likely due to the applied modulation technique which is more easily realized with an electric field than with a mechanical stress. Taking into account the magnitude of the electrooptical effect in MNA (Ref. 45) and the sensitivity achievable in electro-optical measurements,<sup>46</sup> we estimate again a difference in sensitivity of more than  $10^6$  for the detection of induced displacements by both methods.

Both examples, the stress experiment by Jorgensen<sup>38</sup> and the electric-field experiment by Graafsma *et al.*,<sup>44</sup> clearly show the limitation of diffraction experiments. Obviously, internal strain is detectable in this way only if conditions are extraordinarily favorable. This is the reason for the only partial work on this subject in the past. The optical method presented in the present paper opens a new way to attack the problem of internal strain.

## ACKNOWLEDGMENTS

The author is indebted to D. Brach and J. Kushauer for the measurement of some piezo-optical constants.

- <sup>1</sup>M. Born and K. Huang, *The Dynamical Theory of Crystal Lattices* (Oxford University Press, Oxford, 1966).
- <sup>2</sup>Examples are noted in Refs. 5–9; for a recent experimental work showing evidence for the importance of internal strain, see, K. Reimann and K. Syassen, *Solid State Commun.* **76**, 137 (1990).
- <sup>3</sup>For a review of theories in crystals with the diamond structure, see, C. Cousins, *J. Phys. C* **15**, 1857 (1982).
- <sup>4</sup>A. Segmüller and A. R. Neyer, *Phys. Kondens. Mater.* **4**, 63 (1965).
- <sup>5</sup>C. Cousins, *J. Phys. C* **11**, 4867 (1978).
- <sup>6</sup>C. Cousins, *J. Phys. C* **11**, 4881 (1978).
- <sup>7</sup>C. Cousins, *J. Phys. C* **14**, 1585 (1981).
- <sup>8</sup>S. Devine, *J. Phys. C* **16**, 5553 (1983).
- <sup>9</sup>M. Catti, *Acta Crystallogr. A* **45**, 20 (1989).
- <sup>10</sup>*International Tables for Crystallography*, edited by T. Hahn (International Union of Crystallography, Dordrecht, 1987).
- <sup>11</sup>C. Cousins, *Acta Crystallogr. A* **39**, 257 (1983).
- <sup>12</sup>C. Cousins, *J. Appl. Crystallogr.* **21**, 4496 (1988).
- <sup>13</sup>C. Cousins *et al.*, *J. Appl. Crystallogr.* **15**, 154 (1982).
- <sup>14</sup>H. d'Amour, W. Denner, H. Schulz, and M. Cardona, *J. Appl. Crystallogr.* **15**, 148 (1982).
- <sup>15</sup>C. Cousins *et al.*, *J. Phys. C* **15**, L651 (1982).
- <sup>16</sup>C. Koumelis, G. Zardas, C. Londos, and D. Leventuri, *Acta Crystallogr. A* **32**, 84 (1975).
- <sup>17</sup>M. Cardona, K. Kunc, and R. Martin, *Solid State Commun.* **8**, 1205 (1982).
- <sup>18</sup>C. Cousins, *Acta Crystallogr. A* **40**, 116 (1984).
- <sup>19</sup>J. Phillips, *Phys. Rev. Lett.* **20**, 550 (1968).
- <sup>20</sup>J. V. Vechten, *Phys. Rev.* **182**, 891 (1969).
- <sup>21</sup>B. Levine, *Phys. Rev. B* **7**, 2600 (1973).
- <sup>22</sup>C. Shih and A. Yariv, *J. Phys. C* **15**, 825 (1982).
- <sup>23</sup>D. Chemla, *Phys. Rev. Lett.* **26**, 1441 (1971).
- <sup>24</sup>H.-J. Weber, *Z. Kristallogr.* **177**, 185 (1986).
- <sup>25</sup>H.-J. Weber, *Z. Kristallogr.* **177**, 201 (1986).
- <sup>26</sup>H.-J. Weber, *Acta Crystallogr.* **A44**, 320 (1988).
- <sup>27</sup>H.-J. Weber *et al.*, *J. Phys. Condens. Matter* **1**, 8543 (1989).
- <sup>28</sup>B. Levine, *J. Chem. Phys.* **59**, 1463 (1973).
- <sup>29</sup>J. Jerphagnon, D. Chemla, and R. Bonneville, *Adv. Phys.* **27**, 609 (1978).
- <sup>30</sup>J. Nye, *Physical Properties of Crystals* (Oxford University Press, Oxford, 1967).
- <sup>31</sup>E. Fay, H. Völlenkne, and A. Wittmann, *Z. Kristallogr.* **138**, 439 (1973).
- <sup>32</sup>H.-J. Weber, *Mater. Res. Bull.* **17**, 1313 (1982).
- <sup>33</sup>B. Harbrecht, J. Kushauer, and H.-J. Weber, *Eur. J. Solid State Inorg. Chem.* **27**, 831 (1990).
- <sup>34</sup>J. Robertson, *J. Phys. C* **12**, 4767 (1979).
- <sup>35</sup>D. Roessler and J. W. A. Albers, *J. Phys. Chem. Solid* **33**, 293 (1972).
- <sup>36</sup>M. Stapelbroek and B. Evans, *Solid State Commun.* **25**, 959 (1978).
- <sup>37</sup>H. Wang and G. Simmons, *J. Geophys. Res.* **78**, 1262 (1973).
- <sup>38</sup>J. Jorgensen, *J. Appl. Phys.* **49**, 5473 (1978).
- <sup>39</sup>R. Young and B. Post, *Acta Crystallogr.* **15**, 337 (1962).
- <sup>40</sup>W. R. Cook *et al.*, in *Piezoelectric and Electrooptic Constants*, edited by K.-H. Hellwege, Landolt-Börnstein, New Series, Group III, Vol. 11 (Springer-Verlag, Berlin, 1979), p. 520.
- <sup>41</sup>W. Baur and A. Khan, *Acta Crystallogr. B* **27**, 2133 (1971).
- <sup>42</sup>R. Shannon, *Acta Crystallogr. A* **32**, 751 (1976).
- <sup>43</sup>J. Ziolkowski, *J. Solid State Chem.* **57**, 269 (1985).
- <sup>44</sup>H. Graafsma *et al.*, *Acta Crystallogr. A* **48**, 113 (1992).
- <sup>45</sup>G. Lipscomb, A. Garito, and R. Narang, *J. Chem. Phys.* **75**, 1509 (1981).
- <sup>46</sup>H. Becker, D. Brach, A. Otto, and H.-J. Weber, *Rev. Sci. Instrum.* **62**, 1196 (1991).